Resolution enhancement using a multi-layered Aluminum- based plasmonic device for chikungunya virus detection

Sambhavi Shukla
Birla Institute of Technology and Science, Pilani
Nitika Grover
Vellore Institute of Technology University
Pankaj Arora (pankaj.arora@pilani.bits-pilani.ac.in)
Birla Institute of Technology and Science, Pilani

Research Article

Keywords: Aluminum, Surface plasmon, MDM, MoS2, Communication band, and Optical sensor

Posted Date: June 21st, 2022

DOI: https://doi.org/10.21203/rs.3.rs-1752532/v1

Additional Declarations: No competing interests reported.

Version of Record: A version of this preprint was published at Optical and Quantum Electronics on February 1st, 2023. See the published version at https://doi.org/10.1007/s11082-022-04485-y.

Abstract

Biomolecular variations can be accounted for by changes in the intrinsic properties of the surrounding medium, such as the refractive index. This work employs such an arrangement using a modified attenuated total internal reflection configuration for telecommunication wavelength (1550nm). The phenomenon of surface plasmon resonance is initiated by Aluminum (Al) metal due to its low cost and better compatibility with CMOS devices. To achieve improved plasmonic response in terms of the sensor's resolution, we have explored metal-dielectric-metal configuration under angle interrogation. Barium titanate and Molybdenum disulfide (MoS_2) have been employed as the high dielectric constant material and the binding media respectively to enhance the sensing performance. After a series of optimizations, the proposed device configuration leads to a maximum Figure of Merit (FOM) of 540.9 RIU^{-1}, thus enhancing the resolution. The proposed plasmonic device can be used for chikungunya virus detection by considering different blood components in normal and infected stages. This Al-based multi-layered plasmonic device can serve many applications for resolution enhancement in the near-infrared region.

1. Introduction

The cumulative oscillation of conduction electrons at the metal-dielectric interface gives rise to the Surface Plasmon Resonance (SPR) phenomenon under the excitation of TM polarized light. SPR-based label-free sensing technique has proved to become a potential alternative for applications like cancer detection (Gade et al. 2022), food safety (Khansili et al. 2018), enzyme detection (Pumera 2011), etc. Such optical sensors based on the phenomenon of SPR utilize prism-based Kretschmann configurations or periodic nanostructures to excite the Surface Plasmons (SPs). Corresponding to the minute variations of an unknown analyte, optical characteristics are studied in terms of reflection, transmission, and absorption characteristics. Several metals like Silver (Ag), Gold (Au), and Aluminum (Al) are the ones aiding plasmonic resonance at the interface. Among them, Al has become quite an area of interest due to its low cost as well as better plasmonic response in terms of narrow linewidth. Maximum penetration depth, shown by Al, at higher wavelengths is also an attractive advantage in terms of sensitivity over other counterparts like Au and Ag (Prabowo et al. 2019). For the spectral analysis of such a plasmonic device, the near-infrared (NIR) spectrum provides a transparent window toward a majority of biological tissues (Ziblat et al. 2006), unlike the visible region. This paves the way for non-destructive medical diagnosis. On that account, exploring Al-based plasmonic devices in the NIR region for biosensing applications can be perceived as an interesting way to strive for promising results. So far, myriad combinations have been reported over the conventional metal-analyte-based Kretschmann configuration to achieve high-performance yielding parameters. For example, employing high dielectric constant materials like Silicon (Si), PMMA, and Barium Titanate ($BaTiO_3$) also known as BTO, for improved SPR sensitivity, using different material substrates to identify the change in the position of the resonance dips (Moznuzzaman et al. 2021), having metal-dielectric-metal (MDM) designs for field confinement (Zekriti et al. 2015), or utilizing 2D nanomaterials (Graphene, MoS_2, MXene) for increased affinity towards

biomolecules (Shukla and Arora 2021). Thus, a rational miniaturized design can bring about feasibility, improved detection accuracy, and reduced cost for large-scale production.

Out of the silver-based SPR configurations, which considered the dielectric properties of BTO, sensitivity improved substantially but at the cost of compromising the Figure of Merit (FOM) (Srivastava et al. 2020) (Sun et al. 2019)(Vasimalla et al. 2021). Also, in a gold-based sensor employing BTO, FOM was observed to be as low as 37.22 RIU^{-1} (Mostufa et al. 2022). Furthermore, several multi-layered geometries also reported enhanced sensitivity. However, FOM was largely ignored in almost all such modified Kretschmann arrangements. For example, in a bimetallic Ag-Au design, angle interrogation showed sensitivity improvement by 37°/RIU in the case of bimetal w.r.t single metal (Karki et al. 2022b). Among the MDM configurations utilizing BTO, Karki et al have demonstrated an exhaustive sensitivity analysis for Au, Ag, and Copper (Cu) metal layers at 633nm with and without BTO, wherein the stability and sensitivity issues associated with the single metal layered design was reported to be overcome by a bimetallic design (Karki et al. 2022a). Many Au and Ag-based MDM structures are also reported for better sensing performance parameters w.r.t. conventional single metal layer-based SPR sensor in the visible region for either angle interrogation or wavelength interrogation (Liang et al. 2019) (Refki et al. 2018).

Therefore, all these works claimed to have reached for enhanced sensitivity in the visible region by either employing BTO or utilizing the MDM configuration, however, at the cost of neglecting the FOM. This brings us to a dualistic approach for the present work, i.e., considering multi-layered Al-based Kretschmann configuration firstly, over the conventional single metal design in the NIR region. Secondly, to study resolution enhancement in Al-based MDM configuration comprising BTO as the high dielectric constant material thus utilizing the strong field confinement at the interface. Calculating FOM is a sufficient and necessary analysis that considers both the performance parameters, i.e., the sensitivity (S_{max}) of the proposed sensor and the linewidth of the SPR curves. This way, we can come up with a complete and exhaustive study of FOM comparison with the previously reported works. Since utilizing an MDM configuration leads to the reduced linewidth of SPR curves, the FOM is boosted significantly. The entire simulations are performed for angle interrogation at telecommunication wavelength (1550nm) employing the Transfer Matrix Method (TMM). After successive optimization of the intermediate layers, a 2D nanomaterial (MoS_2) is considered for the biofunctionalization of the Al metal. A high absorption coefficient and a narrow linewidth in the NIR region are some of the appealing properties of MoS_2. Analysis of the blood profile for the detection of the chikungunya virus is shown in the last section to capture minute changes in the infected and normal blood components. The chikungunya virus is transmitted by the bite of infected female mosquitoes from one human body to another, especially affecting older people and people with serious health issues. The disease can severely increase morbidity and neurological manifestations as has been reported earlier (Brighton 1981). Since the refractive index of blood depends on the changes in the concentration of its constituents (RBC, plasma, platelets), the normal and infected blood components can be accounted for by changes in the SPR dips due to changes in the refractive index. Finally, on comparing the results of the proposed device with the previously reported works, a significant improvement in the value of FOM in the NIR region is achieved by utilizing

the MDM configuration. The proposed novel SPR sensor can very well be employed in the biomedical domain for varying levels of nanoscale detection.

2. Results And Discussions

Figure 1(a) shows the schematic of the proposed plasmonic device using a conventional Kretschmann configuration, wherein CaF_2 (n = 1.426) glass prism is considered as the substrate and Al is considered as the plasmonic metal. Due to better rejection of errors during mechanical setup as well as a higher threshold for laser damage, the CaF_2 prism is used as the material substrate for angle interrogation. Over a 25nm thick Al film (t_{m1}), BTO (t_{BTO} = 10nm) is deposited as a dielectric material to increase the sensitivity. Thereafter, the second film of Al (t_{m2} = 10nm) is deposited again to get the MDM configuration, thus intensifying field confinement. MoS_2 is used as a biorecognition element (BRE) layer for the analyte under test. The overall fabrication procedure for the proposed device is easy to achieve. With techniques such as e-beam evaporation/thermal evaporation, Al can be deposited on the CaF_2 prism. In between two metal layers of Al, BTO can be deposited using methods like MOCVD or sol-gel method, etc. There are detailed experimental reports for the deposition of BTO over Al films for the application of thin-film capacitors (Ramesh et al. 2003). Above the second Al metal layer, monolayer MoS_2 can be deposited using techniques such as chemical vapor deposition.

Drude's model is used to calculate the dielectric constant for Al using Eq. (1)

$$\varepsilon_m(\lambda) = 1 - \left(\frac{\lambda^2 \lambda_c}{\lambda_p^2 (\lambda_c + j\lambda)} \right) \quad (1)$$

where λ is the wavelength in μm, λ_p = 1.0657e^{-7}m and λ_c= 2.4511 e^{-5}m denote the plasma wavelength and collision wavelength respectively (Arora and Shukla 2020). The refractive index for BTO is calculated from the experimental values reported by Cardona (1965). The refractive index for the MoS_2 monolayer (0.65nm) is extracted from Ref. (Shukla and Arora 2021). The analyte 'n_a' is considered as water over which the change in SPR angle is observed. When a TM-polarized light strikes the metal surface, thereafter, under momentum matching conditions, maximum absorption of incident light is accounted for with points of reflection minima. The reflection characteristics for the proposed device calculated using TMM Method are shown in Fig. 1 (b) where the dip in the reflectivity curve is due to the SP excitation at the interface. A redshift in the SPR curve is noticed with the increase in the analyte's refractive index from 1.33 to 1.34. To quantify the performance parameters of the proposed device, Full Width at Half Maximum (FWHM) and Sensitivity (S_{max}) are calculated which corresponds to the linewidth of the SPR curves and shift in SPR angle w.r.t the change in the refractive index of the analyte (n_a), respectively. Finally, considering both the parameters, FOM, i.e. ratio of S_{max} and FWHM is found to be 540.9 RIU^{-1}.

To get the optimized parameter for all the intermediate layers of the proposed device, several simulations are carried out using the TMM method considering low FWHM of SPR curves, and high signal contrast

(low value of R_{min}) as decisive parameters. Firstly, a conventional Kretschmann configuration with thin Al metal (t_{m1}) coated with an analyte is considered as shown in the inset of Fig. 2(a), and the thickness of Al film (t_{m1}) is varied from 15nm to 35nm in steps of 10nm. The calculated reflection characteristics are shown in Fig. 2(a). It is observed that the reflectivity dip corresponding to 25 nm strives for efficient SP excitation due to high signal contrast (low value of R_{min}) whereas the value of t_{m1} = 15 nm and 35 nm leads to poor signal contrast. Figure 2(b), shows the electric field distribution for t_{m1} = 25 nm, where the excitation of SP mode can be observed with stronger field enhancement at the interface as compared to t_{m1} = 15 nm and 35 nm (not shown here).

Next, a high dielectric constant material 'BTO' is considered on the top of the Al thin metal layer (t_{m1} = 25nm), and reflection characteristics are calculated with the variation in the thickness of BTO material (t_{BTO}) over a range of 5nm to 15nm as shown in Fig. 3(a). It can be seen that the signal contrast (value of R_{min}) is almost constant with the variation in the thickness of the BTO layer. Since the high dielectric constant of BTO leads to enhanced sensitivity, the sensitivity and FOM are chosen to be the decisive parameters to get the optimized value of t_{BTO}. To calculate the sensitivity and FWHM from SPR curves, the refractive index of the analyte is varied from 1.33 to 1.34. An increase in the redshift is observed with the changing analyte's index as we keep on increasing the BTO thickness. It is also observed that with the increase in the BTO thickness (t_{BTO}), the FWHM is also increasing. Therefore, a trade-off is established between sensitivity (S_{max}) and FOM over a varying thickness of BTO (t_{BTO}) as shown in Fig. 3(b). A value of 10 nm for the thickness of the BTO layer is found to be the optimized one for a decent value of sensitivity and FOM. The comparison among the respective values of sensitivity and FOM with the variation in t_{BTO} can be seen subsequently in Table 1 below.

Table 1
COMPARISON OF PERFORMANCE PARAMETERS WITH INCREASE IN THICKNESS OF BTO LAYER

t_{BTO} [nm]	S_{max} [°/RIU]	FWHM [°]	FOM [RIU^{-1}]	R_{min}
5	121	0.51	237.2	0.026
10	**124**	**0.54**	**229.6**	**0.028**
15	128	0.64	200	0.030

After optimizing the thicknesses of the Aluminum thin metal layer (t_{m1} = 25nm), and BTO layer (t_{BTO} =10nm), we have considered another Al metal layer of thickness t_{m2} deposited on the BTO layer to achieve MDM configuration. The reflection characteristics are calculated with the variation in the thickness of the second Al metal layer (t_{m2}) over a range of 5nm to 15nm, as shown in Fig. 4(a). To calculate the sensitivity and FWHM from SPR curves, the refractive index of the analyte is varied from 1.33 to 1.34. Although the sensitivity is observed to be almost constant with the increase in thickness of

the second Al metal layer (t_{m2}), the FWHM is found to be decreasing, resulting in improved FOM or the resolution of the sensor. A decrease in the signal contrast (value of R_{min}) is also observed with increasing the second Al metal layer thickness(t_{m2}). To have a decent value of signal contrast and FWHM, a trade-off between the R_{min} and FWHM is established with the variation in the thickness of the second metal layer (t_{m2}) as shown in Fig. 4(b). An optimized value of t_{m2} = 10 nm is noticed for a decent value of signal contrast and FWHM for the proposed MDM configuration. The comparison among the respective values of Rmin, FWHM, and FOM with the variation in t_{m2} can be seen subsequently in Table 2 below.

Table 2
COMPARISON OF PERFORMANCE PARAMETERS WITH INCREASE IN THICKNESS OF SECOND Al METAL LAYER (t_{m2})

t_{m2} [nm]	S_{max} [°/RIU]	FWHM [°]	FOM [RIU^{-1}]	R_{min}
5	120	0.31	390.3	0.049
10	**119**	**0.22**	**540.9**	**0.24**
15	120	0.18	655.5	0.45

The reason for an increased resolution or FOM of the proposed MDM configuration-based plasmonic device can be explained with the help of calculated electric field distribution as shown in Fig. 5. Figure 5(a) shows the electric field distribution for conventional Kretschmann configuration (glass prism + Al metal + analyte), whereas Fig. 5(b) shows the electric field distribution for the proposed Al-based multi-layered plasmonic device with MDM configuration respectively. An enhanced electric field observed in the vicinity of the metal-analyte interface is attributed to the SP mode excitation after the maximum energy transfer from the incident light to SPs (Fig. 5(a)). Eventually, this field interaction gets more localized as soon as the t_{m2} layer is added above the BTO thin film to form an MDM configuration (Fig. 5(b)). The strong field localization results in lower FWHM of the SP curve in the case of MDM configuration (Arora and Krishnan 2013). Such field distribution is directly related to the penetration depth that defines the interaction length of SPs. As a result, a reduced penetration depth in the MDM configuration (a few tens of nanometers) leads to reduced FWHM and thus larger FOM with respect to conventional Kretschmann plasmonic devices having penetration depth of about hundreds of nanometers.

Table 3 compares the effect of each of the intermediate layers in between the glass prism and analyte. Compared to the conventional Kretschmann configuration (Case -I), with the successive addition of the BTO layer (Case-II), sensitivity is improved but at the cost of poor FOM, as already reported in the literature. In the proposed Al-based multi-layered plasmonic device with MDM configuration (Case-III), an enhancement in FOM or resolution is observed due to a reduction in the FWHM of the SP curve at 1550nm.

Table 3
EFFECT OF DIFFERENT LAYERS ON THE PERFORMANCE PARAMETERS OF THE PROPOSED DEVICE

Configurations	S_{max} [°/RIU]	FWHM [°]	FOM [RIU^{-1}]
Case I	118	0.42	280.95
Case II	124	0.54	229.62
Case III	**119**	**0.22**	**540.9**

Finally, to demonstrate biosensing application for the proposed plasmonic device, a monolayer MoS_2 is considered on the proposed device (Fig. 1(a)) as BRE to bind the biomolecules. The better absorptivity nature of this bio-analyte enables its extensive use for biosensing purposes. Since pure Al is not viable for biosensing applications, thus, the MoS_2 layer protects the Al metal layer from oxidation. Figure 6 presents the reflection characteristics of different blood components in normal and infected stages as a bio-analyte on the proposed plasmonic device. The refractive index values for the different blood components are taken from Ref. (Sharma et al. 2021). A blueshift in the SPR curves is observed for all the blood components due to a decrease in the refractive index in the infected stage as compared to the normal stage.

At last, the results obtained from the proposed plasmonic device are compared with the previously published results as shown in Table 4. The obtained FOM is much higher than the recently published results where FOM was largely ignored. Utilizing the cost-effective Al for resolution/FOM enhancement with the proposed MDM configuration in the prism-based plasmonic device can be used as a promising SPR sensor for future applications in the NIR region.

Table 4
FOM COMPARISON OF THE PROPOSED PLASMONIC DEVICE WITH PREVIOUSLY REPORTED WORKS

Schematic	Wavelength [nm]	FOM [RIU^{-1}]	References
Cu + BTO + Cu + BP	633	145	(Karki et al. 2022a)
Ag + BTO + Gr	633	45.05	(Sun et al. 2019)
Ag + Au + BTO + Gr	633	42.13	(Karki et al. 2022b)
Ag + BTO + Ag + Gr	633	54	(Pal and Jha 2021)
Ag + BTO + BP/MoS_2	633	60.52	(setareh and Kaatuzian 2021)
CaF_2 prism + Al + BTO + Al + MoS_2	**1550**	**540.9**	**Proposed work**

3. Conclusions

An Al-based multi-layered plasmonic device was proposed for enhanced resolution for sensing applications in the optical communication band. MDM configuration was introduced in the conventional prism-based plasmonic device to increase the FOM by decreasing the linewidth of SPR curves. The effect of each intermediate layer in the proposed Al-based multi-layered device was carried out by studying the performance parameter analysis from the reflection characteristics. An improved value of FOM with a decent sensitivity is obtained for the proposed plasmonic device, leading to the resolution enhancement. The engineered plasmonic device was then used to demonstrate the bio-sensing application at the optical wavelength of 1550nm. The different blood components were considered in normal and infected stages on the proposed plasmonic device for detecting the chikungunya virus. The proposed plasmonic device can serve many bio-sensing applications for resolution enhancement in the near-infrared region.

Declarations

Competing interests. The authors declare no conflicts of interest.

Availability of Data and materials. The dataset generated or analysed during the current study is available from the corresponding author on reasonable request.

Funding. The authors declare that no funds, grants, or other support were received during the preparation of this manuscript.

Ethics approval and consent to participate. Not applicable.

Consent for publication. All the authors have their full consent for the work submitted in this manuscript.

Authors' Contribution. S.S. and P.A. contributed equally. N.G and P.A. supervised the work and reviewed the manuscript.

Acknowledgments

S.S. and P.A. would like to thank the Birla Institute of Technology and Science, Pilani (Rajasthan), India for providing an Additional Competitive Research Grant (ACRG). The authors would also like to thank Nihal Singh and Vishnu Venkatesh for the fruitful discussions.

References

1. Arora, P., Krishnan, A.: Analysis of transmission characteristics and multiple resonances in plasmonic gratings coated with homogeneous dielectrics. In: Progress in Electromagnetics Research Symposium. pp. 927–931 (2013)
2. Arora, P., Shukla, S.: Self-referenced integrated plasmonic device based on engineered periodic nanostructures for sensing application. In: SPIE proceedings. SPIE (2020)

3. Brighton, S.W.: Chikungunya Virus Infections. South African Med. J. 59, 552 (1981). https://doi.org/10.1056/NEJMc1505501
4. Cardona, M.: Optical properties and band structure of SrTiO3 and BaTiO3. Phys. Rev. 140, (1965). https://doi.org/10.1103/PhysRev.140.A651
5. Gade, A., Sharma, A., Srivastava, N., Flora, S.J.S.: Surface plasmon resonance: A promising approach for label-free early cancer diagnosis. Clin. Chim. Acta. 527, 79–88 (2022). https://doi.org/10.1016/j.cca.2022.01.023
6. Karki, B., Pal, A., Singh, Y., Sharma, S.: Sensitivity enhancement of surface plasmon resonance sensor using 2D material barium titanate and black phosphorus over the bimetallic layer of Au, Ag, and Cu. Opt. Commun. 508, 127616 (2022)(a). https://doi.org/10.1016/j.optcom.2021.127616
7. Karki, B., Uniyal, A., Chauhan, B., Pal, A.: Sensitivity enhancement of a graphene, zinc sulfide-based surface plasmon resonance biosensor with an Ag metal configuration in the visible region. J. Comput. Electron. 36, 1108–1116 (2022)(b). https://doi.org/10.1007/s10825-022-01854-4
8. Khansili, N., Rattu, G., Krishna, P.M.: Label-free optical biosensors for food and biological sensor applications. Sensors Actuators, B Chem. 265, 35–49 (2018). https://doi.org/10.1016/j.snb.2018.03.004
9. Liang, Z., Wen, Y., Zhang, Z., Liang, Z., Xu, Z., Lin, Y.S.: Plasmonic metamaterial using metal-insulator-metal nanogratings for high-sensitive refraction index sensor. Results Phys. 15, 102602 (2019). https://doi.org/10.1016/j.rinp.2019.102602
10. Mostufa, S., Akib, T.B.A., Rana, M.M., Mehedi, I.M., Al-Saggaf, U.M., Alsaggaf, A.U., Alsaggaf, M.U., Alam, M.S.: Numerical approach to design the graphene-based multilayered surface plasmon resonance biosensor for the rapid detection of the novel coronavirus. Opt. Contin. 1, 494 (2022). https://doi.org/10.1364/optcon.445255
11. Moznuzzaman, M., Khan, I., Islam, M.R.: Nano-layered surface plasmon resonance-based highly sensitive biosensor for virus detection: A theoretical approach to detect SARS-CoV-2. AIP Adv. 11, 065023-1-065023–10 (2021). https://doi.org/10.1063/5.0046574
12. Pal, A., Jha, A.: A theoretical analysis on sensitivity improvement of an SPR refractive index sensor with graphene and barium titanate nanosheets. Optik (Stuttg). 231, 166378 (2021). https://doi.org/10.1016/j.ijleo.2021.166378
13. Prabowo, B.A., Hermida, I.D.P., Manurung, R.V., Purwidyantri, A., Liu, K.C.: Nano-film aluminum-gold for ultra-high dynamic-range surface plasmon resonance chemical sensor. Front. Optoelectron. 12, 286–295 (2019). https://doi.org/10.1007/s12200-019-0864-y
14. Pumera, M.: Graphene in biosensing. Mater. Today. 14, 308–315 (2011). https://doi.org/10.1016/S1369-7021(11)70160-2
15. Ramesh, S., Shutzberg, B.A., Huang, C.C., Gao, J., Giannelis, E.P.: Dielectric Nanocomposites for Integral Thin Film Capacitors: Materials design, Fabrication and Integration issues. IEEE Trans. Adv. Packag. 26, 17–24 (2003). https://doi.org/10.1109/TADVP.2003.811365

16. Refki, S., Hayashi, S., Ishitobi, H., Nesterenko, D. V., Rahmouni, A., Inouye, Y., Sekkat, Z.: Resolution Enhancement of Plasmonic Sensors by Metal-Insulator-Metal Structures. Ann. Phys. 530, 1–7 (2018). https://doi.org/10.1002/andp.201700411
17. Setareh, M., Kaatuzian, H.: Sensitivity enhancement of a surface plasmon resonance sensor using Blue Phosphorene/MoS2 hetero-structure and barium titanate. Superlattices Microstruct. 153, 106867 (2021). https://doi.org/10.1016/j.spmi.2021.106867
18. Sharma, S., Kumar, A., Singh, K.S., Tyagi, H.K.: 2D photonic crystal based biosensor for the detection of chikungunya virus. Optik (Stuttg). 237, 166575 (2021). https://doi.org/10.1016/j.ijleo.2021.166575
19. Shukla, S., Arora, P.: Design and comparative analysis of aluminum-MoS2 based plasmonic devices with enhanced sensitivity and Figure of Merit for biosensing applications in the near-infrared region. Optik (Stuttg). 228, (2021). https://doi.org/10.1016/j.ijleo.2020.166196
20. Srivastava, A., Das, R., Prajapati, Y.K.: Effect of Perovskite material on performance of surface plasmon resonance biosensor. IET Optoelectron. 14, 256–265 (2020). https://doi.org/10.1049/iet-opt.2019.0122
21. Sun, P., Wang, M., Liu, L., Jiao, L., Du, W., Xia, F., Liu, M., Kong, W., Dong, L., Yun, M.: Sensitivity enhancement of surface plasmon resonance biosensor based on graphene and barium titanate layers. Appl. Surf. Sci. 475, 342–347 (2019). https://doi.org/10.1016/j.apsusc.2018.12.283
22. Vasimalla, Y., Pradhan, H.S., Pandya, R.J.: Sensitivity enhancement of the SPR biosensor for Pseudomonas bacterial detection employing a silicon-barium titanate structure. Appl. Opt. 60, (2021). https://doi.org/10.1364/ao.427499
23. Zekriti, M., Nesterenko, D. V., Sekkat, Z.: Long-range surface plasmons supported by a bilayer metallic structure for sensing applications. Appl. Opt. 54, 2151–2157 (2015). https://doi.org/10.1364/ao.54.002151
24. Ziblat, R., Lirtsman, V., Davidov, D., Aroeti, B.: Infrared Surface Plasmon Resonance: A Novel Tool for Real Time Sensing of Variations in Living Cells. Biophys. J. 90, 2592–2599 (2006). https://doi.org/10.1529/biophysj.105.072090

Figures

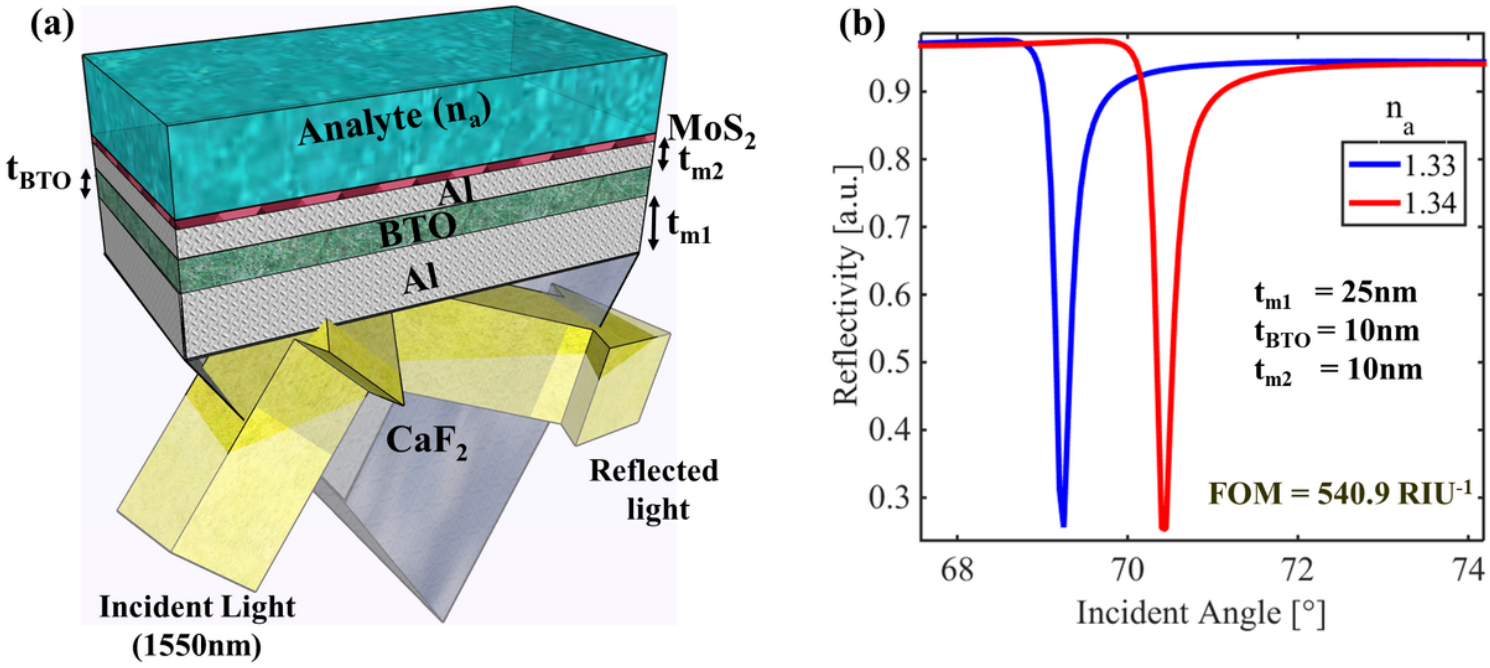

Figure 1

(a) Schematic for the proposed Al-based multi-layered plasmonic device with MDM configuration (b) Reflection characteristics for the proposed device with the redshift in SPR angle due to change in the refractive index of the analyte(n_a).

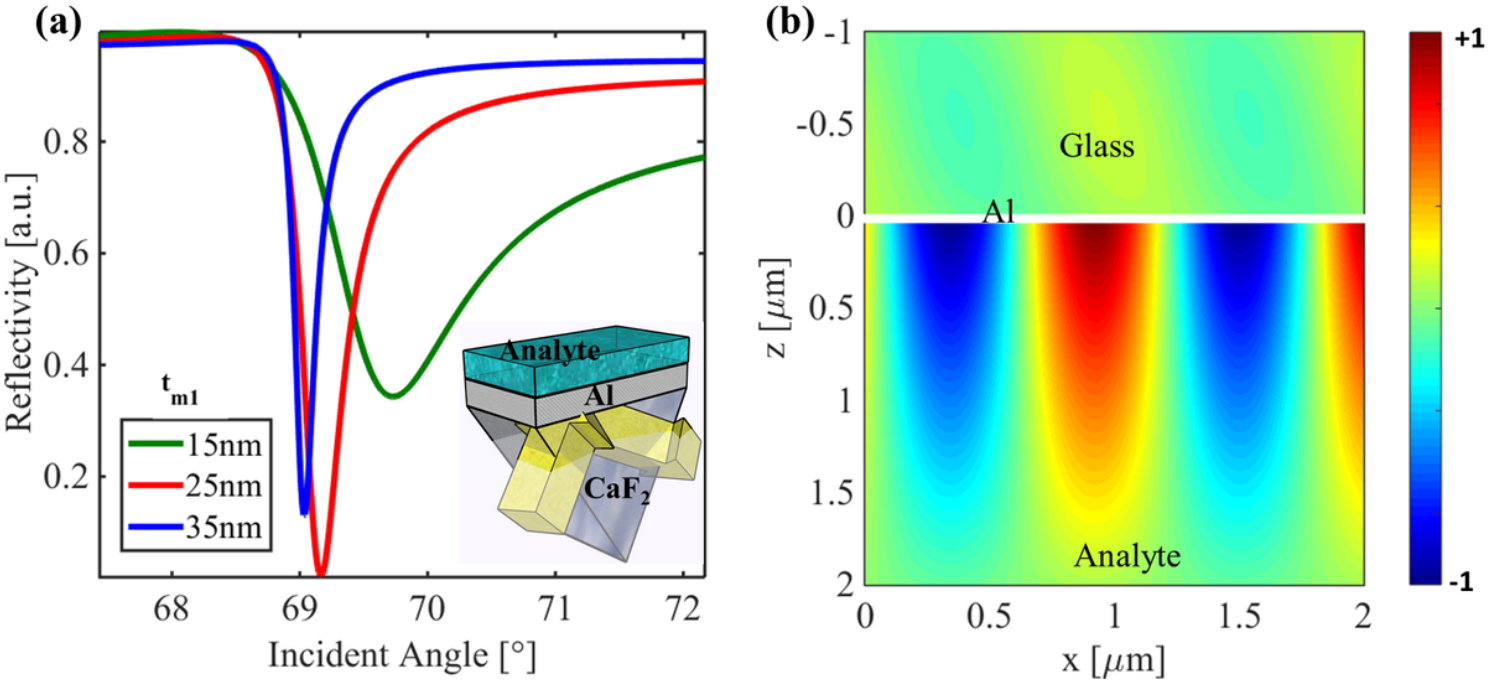

Figure 2

(a) Reflection characteristics for the conventional Kretschmann configuration with the variation in the Al metal thickness (t_{m1}). The inset shows the schematic of the conventional Kretschmann configuration

with a thin Al metal-analyte interface (b) Electric field distribution corresponding to the SP mode for Al metal thickness of t_{m1} = 25 nm.

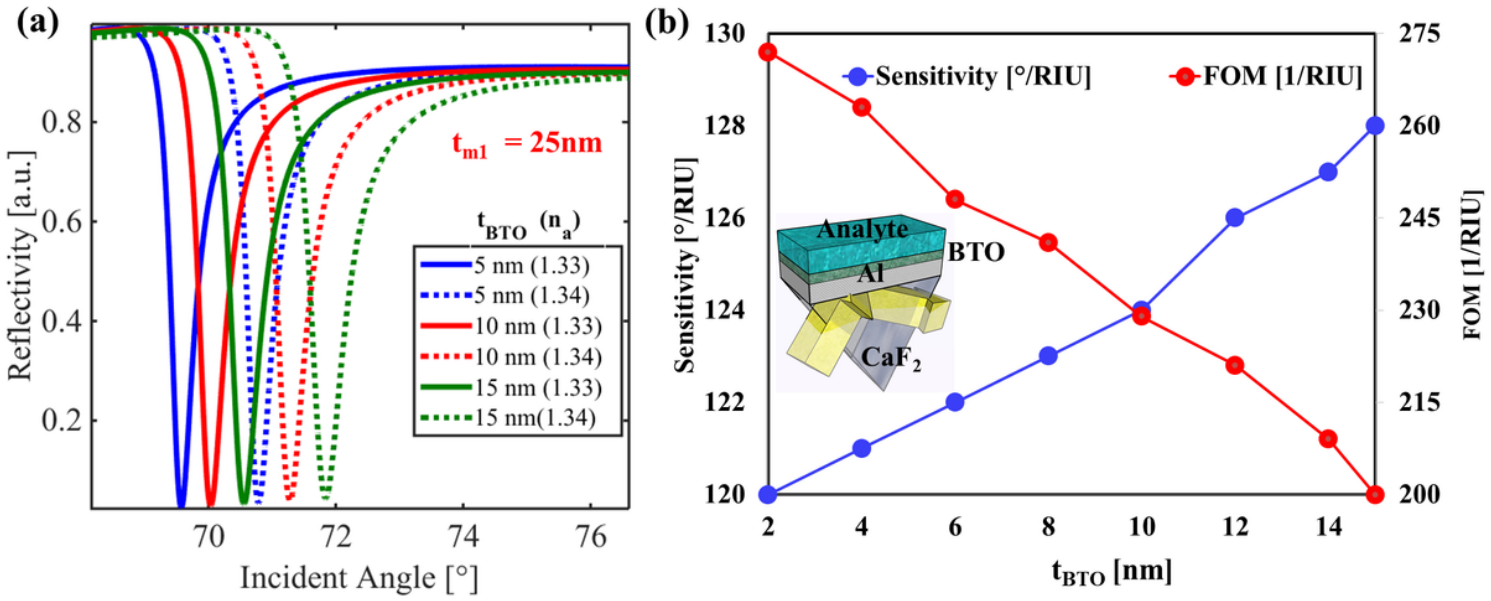

Figure 3

(a) Reflection characteristics with the change in the refractive index of analyte for different thicknesses of BTO layer (b) Trade-off between sensitivity and FOM for varying BTO thickness. Inset shows the schematic of conventional Kretschmann configuration with the addition of BTO layer between thin Al metal layer and the analyte.

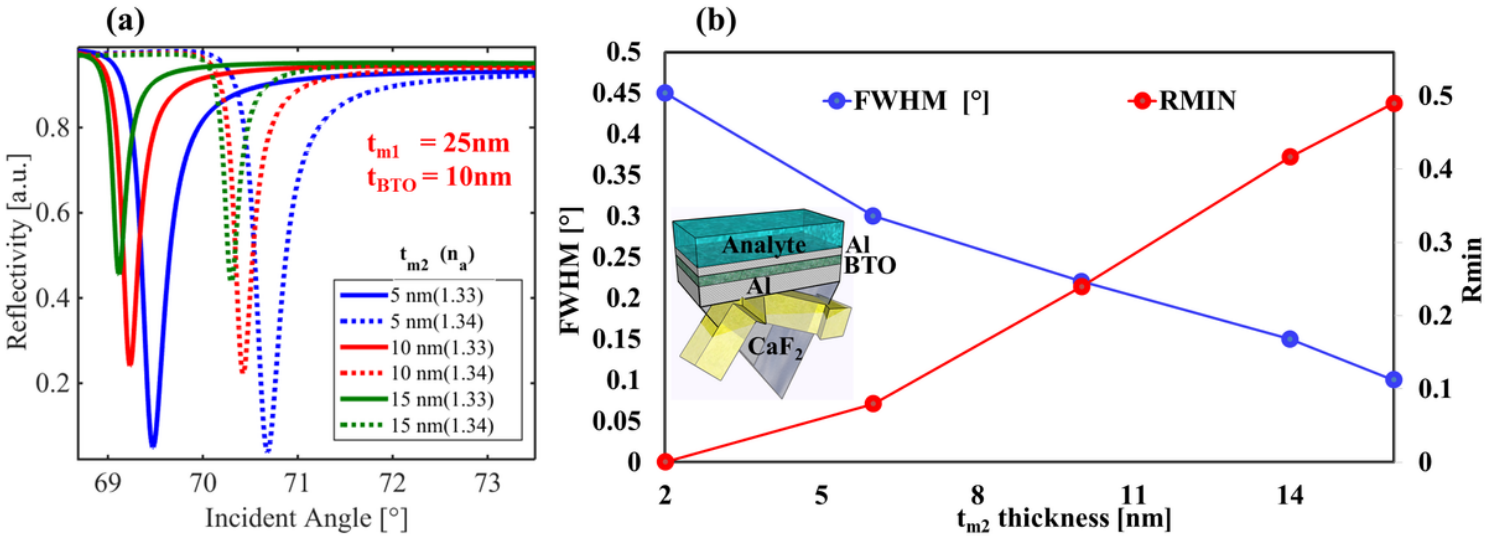

Figure 4

(a) Reflection characteristics with the variation in the refractive index of analyte for different thicknesses of second Al metal layer (t_{m2}) (b) Trade-off between the Rmin and FWHM for different thicknesses of

second Al metal layer (t_{m2}). Inset shows the schematic of the Al-based multi-layer plasmonic device with MDM configuration

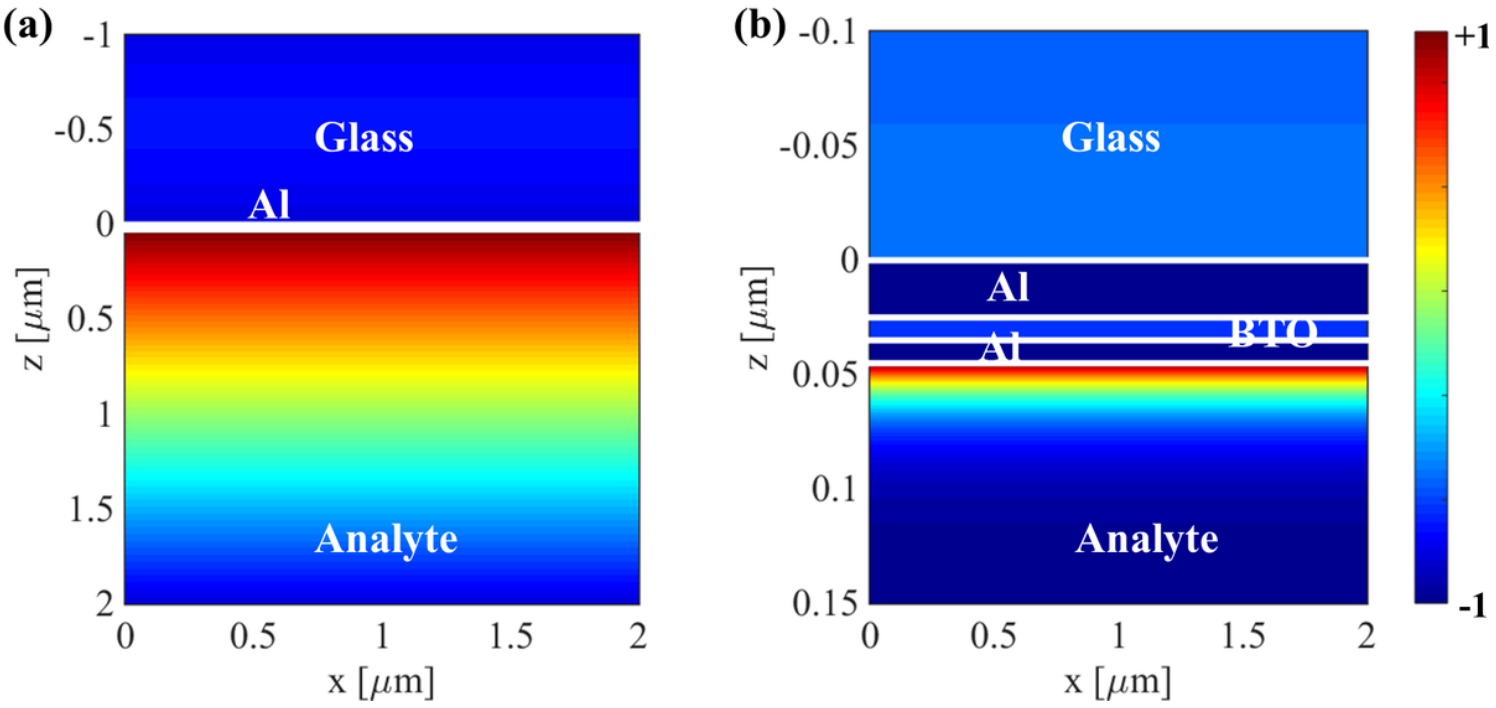

Figure 5

Electric field (E_Z) distributions of the SPR dip for (a) Conventional Kretschmann configuration {Glass + Al metal + Analyte} and (b) the proposed Al-based multi-layered plasmonic device with MDM configuration respectively.

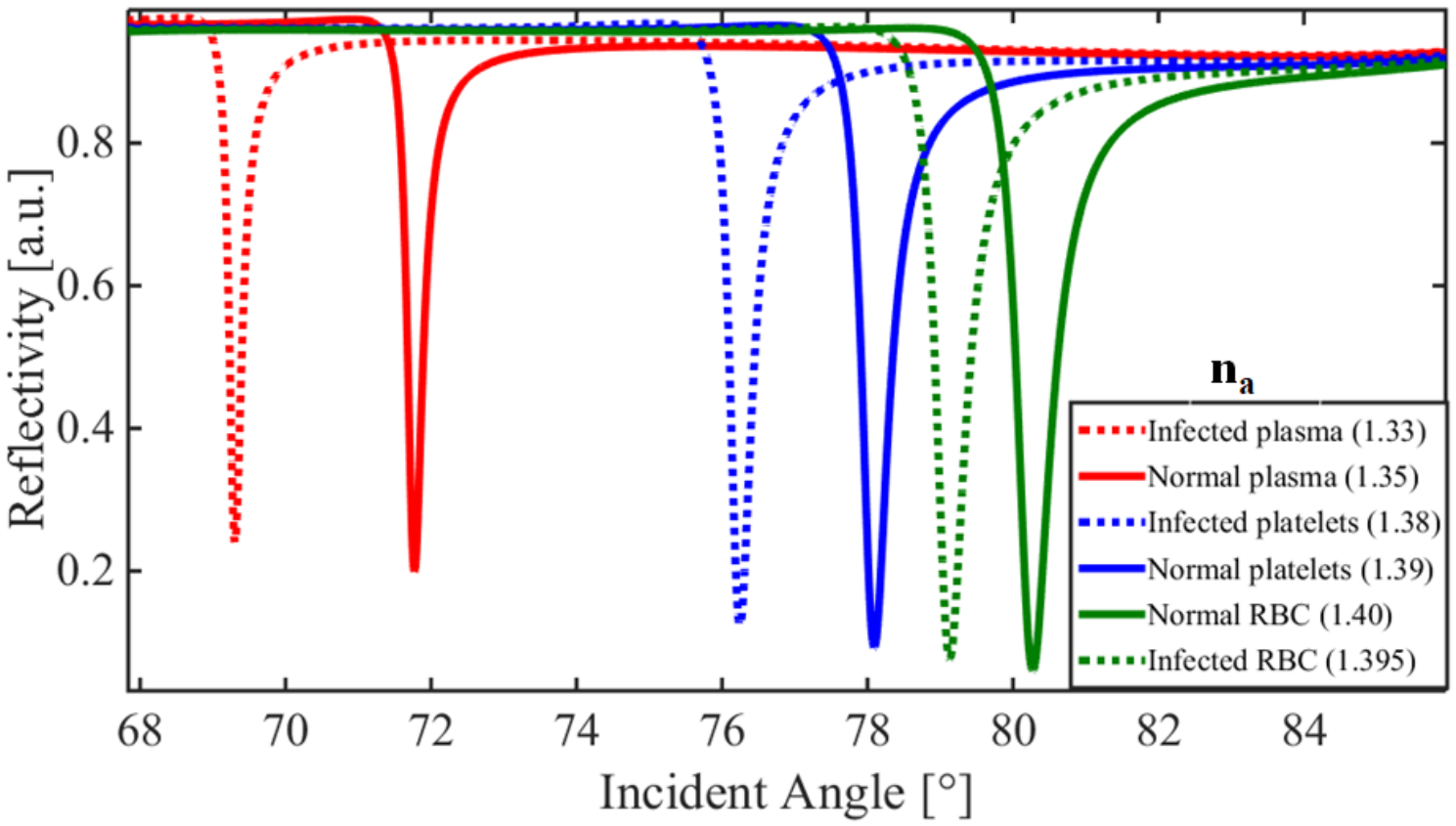

Figure 6

Reflection characteristics of the proposed plasmonic device for different blood components in normal and infected stage